Hamlin, S., Ibraim, E., Lings, M., Muir Wood, D., Cavarretta, I., & Camenen, J-F. (2015). Experimental investigation of wave propagation in three dimensions in unbounded particulate assemblies. In V. A. Rinaldi, M. E. Zeballos, & J. J. Clariá (Eds.), *Deformation Characteristics of Geomaterials: 6th International Symposium on Deformation Characteristics of Geomaterials* (pp. 390-397). (Advances in Soil Mechanics and Geotechnical Engineering; Vol. 6). IOS Press. https://doi.org/10.3233/978-1-61499-601-9-390

Experimental investigation of wave propagation in three dimensions in unbounded particulate assemblies

Simon Hamlin[a], Erdin Ibraim[a], Martin Lings [a], David Muir Wood [b], Ignazio Cavaretta[c], Jean Francois Camenen[d]
[a] *University of Bristol, UK*
[b] *University of Dundee, UK*
[c] *University of Surrey, UK (formerly at University of Bristol)*
[d] *University of Rijeka, Croatia (formerly at University of Bristol)*

Abstract. Understanding wave propagation through soils is essential for site response analysis in earthquake engineering, interpretation of geophysical surveys and SASW (Spectral Analysis of Surface Waves), interpretation of laboratory bender element tests, etc. Analysis of wave propagation has largely been based on continuum descriptions and two dimensional analyses. This study presents recent developments in multiaxial testing that permit the combination of laboratory seismic testing with exploration of three-dimensional principal stress space. A Cubical Cell Apparatus with bender-extender piezoceramic elements fitted in all six faces are used so that wave propagation velocities of an analogue granular material can be determined. The results of a first series of wave propagation tests for a sample under isotropic confinement are presented.

Keywords. Laboratory, cubical cell apparatus, wave propagation

1. Introduction

Predictions of soil movements during construction and operation of many geotechnical systems rely on accurate description of the response of soil at small strain levels. In the laboratory the measurement of stiffness of soils in the small strain domain can be achieved from static or dynamic laboratory tests. Static tests require precise control and measurement of very small stress and strain increments while the dynamic tests like resonant column [1], and the measurements of the body wave velocities within the soil element [2-8] present real challenges in data interpretation ([9], among others) which are based on the theory of wave propagation and require either prior knowledge of a constitutive model for soil or manipulation of continuum medium theory assumptions.

The measurement of body wave velocities is based on the generation at one end of a confined soil sample of an elastic wave produced by piezoceramic bender/extender (B/E) elements [10] which is received at the other end of the sample by other piezoceramic elements, so that shear and compression wave velocities (and corresponding stiffnesses) can be determined non-destructively and relatively fast. Recent studies [11], including numerical analysis of wave transmission [9], leave questions regarding the optimum nature of the input signal, identification of travel time, effect of boundary reflections.

This paper explores some recent developments in multiaxial testing that permit the combination of laboratory geophysics with exploration of principal stress space. A Cubical Cell Apparatus (CCA) with piezoceramic elements fitted in the faces are used so that wave propagation velocities of an analogue granular material made of uniform spherical glass beads can be determined. The results of a first series of wave propagation tests for a sample under isotropic confinement are presented.

1.1. Cubical Cell Apparatus

Incremental stiffness of soil depends on the nature of the particles, state of packing, stress state and strain history. Soil fabric is usually anisotropic – gravitational deposition leads to initial anisotropy, and additional anisotropy is induced by stress history. Most studies of soil stiffness have worked with the axisymmetric triaxial cell which has two degrees of freedom and provides very limited possibilities of exploration of stress space. In practice, elements of soil in the ground or around geotechnical systems will experience variations of six independent stress variables. The torsional hollow cylinder apparatus provides the possibility of controlling four of the six degrees of freedom but at the expense of radial variation of stress and strain components through the thickness of the wall of the sample. True triaxial apparatus (Figure 1a) provide the possibility of controlling the magnitude of the three principal stresses and strains under relatively well preserved uniformity of stresses and strains within cuboidal sample, thus approaching a little closer to the six degrees of freedom of a general stress state. The results presented here come from experiments conducted in a flexible boundary cubical cell (Cubical Cell Apparatus - CCA, [12]) which has been built at the University of Bristol [13]. A general view of the CCA is shown in Figure 1b, while the sample (10x10x10 cm^3 volume) contained in a latex rubber bag is shown in Figure 2.

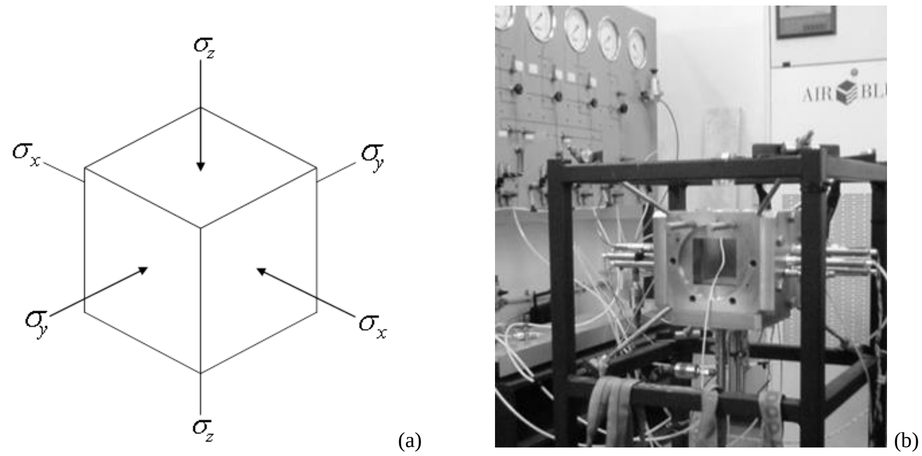

Figure 1. (a) True triaxial apparatus: independent control of three principal stresses. (b) Cubical Cell Apparatus.

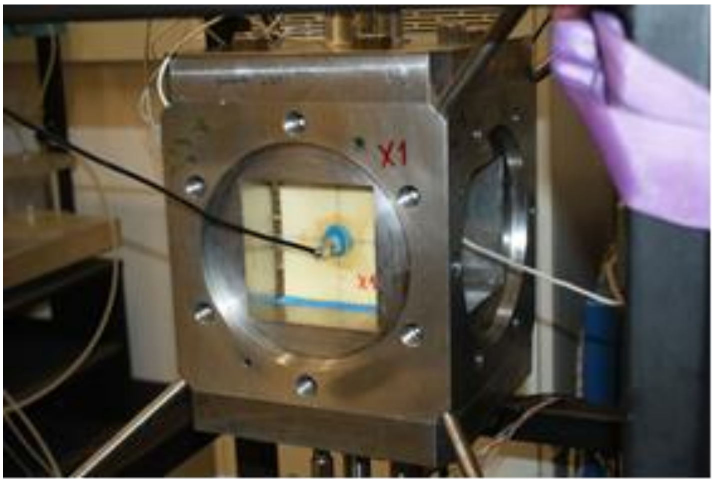

Figure 2. Installation of the cubical sample into the apparatus.

The soil sample is supported by flexible ‘top-hat’ shaped air-filled cushions clamped into the sides of a cubical frame. Opposite pairs of cushions are connected so that changes in the applied stresses are synchronized. Three LVDTs are used on each of the six faces for the measurement of the displacements, while the pressures in the cushions are measured with pressure transducers located immediately behind cushions.

1.2. Material and sample preparation

Stress controlled isotropic compression tests have been performed on dry ballotini glass particles. The borosilicate glass ballotini with a solid density of 2.23 g/cm^3 and with nominal diameters between 2.4mm and 2.7mm were tested. This material is almost mono-disperse and the coefficient of uniformity $U = d_{60}/d_{10}$ is 1.02. Detailed characterisation of the shape of the particles as well as particle-scale mechanical measurements have been conducted by [14].

The samples are prepared by pluviation into a membrane held by vacuum against the sides of a cubical mould. A special pluviation device for fabrication of cubical samples of granular materials designed also to allow the control of the height of fall has been developed. A schematic view of its functioning principle is shown in Figure 3, while detailed analysis of sample quality produced by the pluviation process can be found in [15]. Once full, the top of the sample was carefully sealed and a thin tube was subsequently used to establish a vacuum of about 50 kPa in the sample. This provided sufficient effective stress within the glass material for it to be stiff enough to be lifted in its containing membrane from the mould and locate it in the cubical cell (Figure 2).

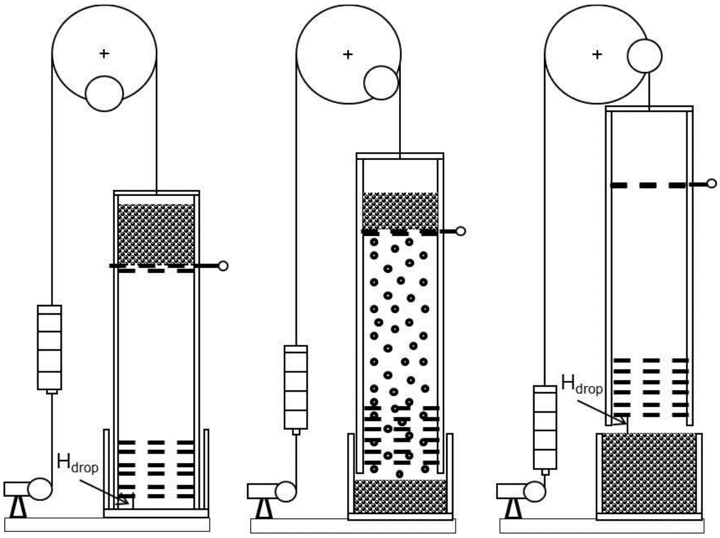

Figure 3. Schematic functioning principle of the pluviation device.

1.3. Wave propagation technique

A piezoelectric material generates electrical output when subjected to mechanical deformation or vice versa and changes its shape when an electrical field is applied to it. Based on the technique developed by [10], pairs of Bender/Extender (B/E) elements have been manufactured and mounted in all six faces of the CCA sample for body wave propagation velocity assessment of the testing material. The B/E element consists of two bimorph piezo-ceramic plates. Each B/E element is coated with epoxy and a pair of them encapsulated in a T-shaped form into a cylindrical plug using resin (Figure 4a). The dimension of the cantilever part of the B/E element, which penetrates the soil, is approximately 5x5x0.51mm. A bender transmitter requires a three-wire parallel connection while the bender receivers have a two-wire series connection and opposite-sense polarised plates. By changing the parallel wired connection to series one, the bender transmitter becomes an extender receiver and the same principle applies for the series connection, when it is changed to parallel connection while keeping the opposite-sense polarised plates, then the bender receiver is switched to an extender transmitter and the resulting motion changes from cantilever bending to longitudinal tension and contraction [10]. Electronic amplification signals, a wave form function generator and a high resolution oscilloscope complete the measurement chain.

The installation of the B/E elements represents a critical and delicate step as penetration of the latex membrane in the center of the faces through a T-shaped cut having exactly the same size and shape as the B/E element should avoid any loss of the vacuum. In the process, a sealing grommet guides the cylindrical body that houses the T-shaped pair of B/E elements (Figure 4b), while several latex layers of adhesive solution are then applied to the grommet-membrane boundary to ensure the sealing of the sample. In a normal wave propagation investigation all types of body and shear waves can be transmitted along the principal sample directions.

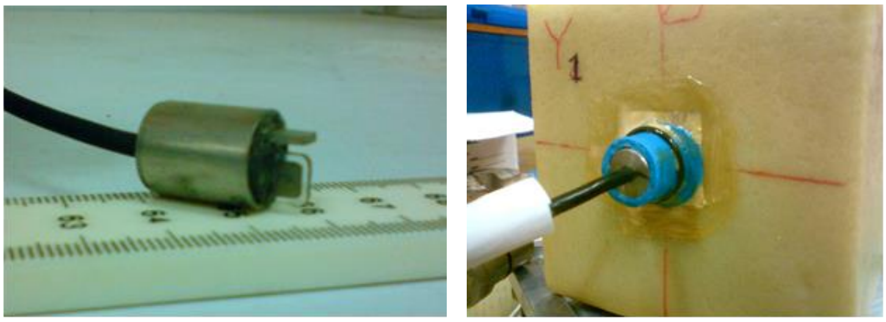

(a) (b)

Figure 4. (a) Picture of the T-shaped B/E system. (b) Installation of the B/E element into the sample.

2. Experimental results

Experimental results are presented for a test on a pluviated assemblage of 2.4-2.7 mm borosilicate glass beads loaded isotropically to 500 kPa in the CCA, with bender/extender elements on all three axes of the CCA. The axial stress-strain results are shown in Figure 5 and show that the pluviated cross-anisotropic fabric has slightly rotated so that the Y – horizontal - and Z – vertical – axes are broadly symmetrical while the X - horizontal axis is different showing a marginally stiffer stress-strain response; this is presumed to be caused by some disturbances in the sample during bender/extender installation processes amplified by the coarse size of the tested material. Further investigation on this issue, which hasn't been observed for fine graded granular particles, is in progress.

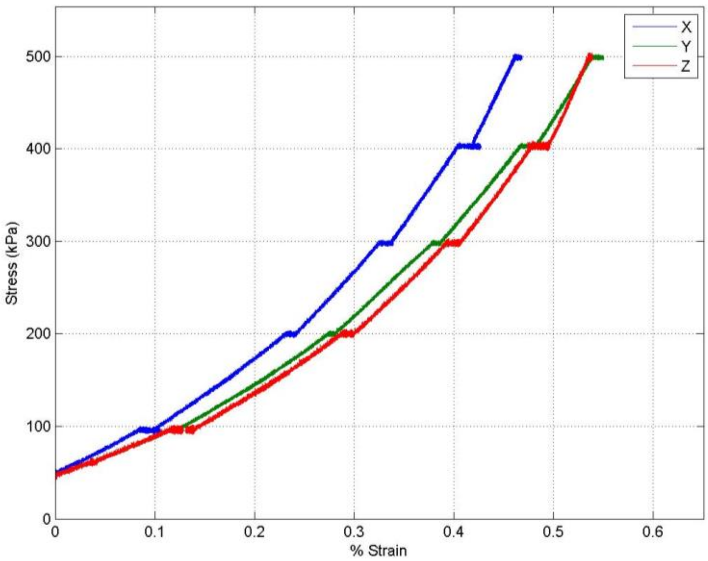

Figure 5: Axial stress-strain curves during isotropic loading; direction of X, Y, and Z axes as shown in Figure 1a.

Wave transmission tests were carried out during isotropic loading at 50 kPa (the pressure of the internal vacuum applied to the sample during fabrication) and 100 kPa followed by 100 kPa increments up to 500 kPa. The transmitted signal was a single sinusoid with a function frequency of 15 kHz and a 270º phase angle, giving us a single peak only (Figure 6). The wave travel time is measured as the time offset between the transmitted peak and the first positive peak in the received signal, termed peak-to-peak (P2P). A nomenclature for velocity of the form 'V_{xy}' is adopted, where 'V' denotes velocity, the first subscript indicates the axis of wave propagation and the second denotes the direction of polarisation (so both subscripts indicate the plane of wave polarisation). 'V_{xy}' therefore denotes an S-wave propagating in the direction of the X axis and polarised in the XY plane. For P-waves the directions of propagation and oscillation are the same, so the subscript is repeated (e.g. 'V_{xx}').

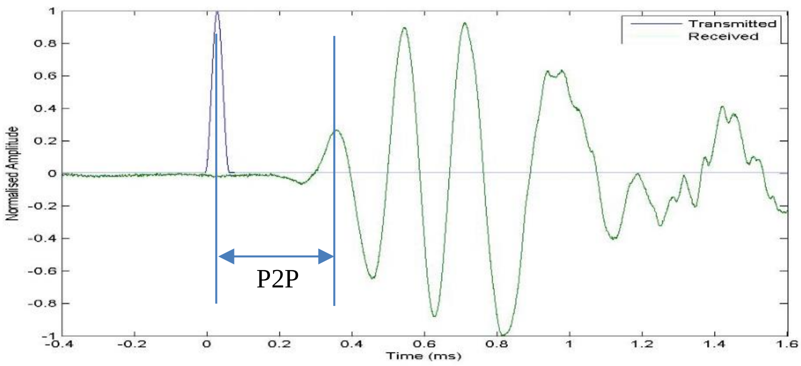

Figure 6: Example transmitted and received S-wave propagating on the Y-axis and polarised in the XY horizontal plane.

The calculated wave velocities as a function of mean effective pressure p' are shown in Figure 7 (P-waves) and Figure 8 (S-waves). As expected, the velocities increase with the effective pressure following power laws. The effective medium theory (EMT) used to describe sound propagation in granular media predicts that the ultrasound velocity V_s should depend on the applied consolidation stress according to the equation: $V_s \alpha\ (p')^n$. In the case of Hertzian contacts between elastic spherical particles, $n = 1/6$. However, in disordered assemblies of spheres, the experimentally obtained power law exponent is higher between 1/4 and 1/3, while [16] showed that for assemblies of particles with conical contacts instead of spherical, n = 1/4. The P-wave results show V_{yy} and V_{zz} are similar while V_{xx} is slightly greater, which conforms to the stress-strain results in Figure 5 where the X-axis shows a stiffer response. However, the power coefficients are similar, around 0.20. The results for S-waves, however, are more complex most probably due to some dependence of the S-wave velocity on the sample fabric properties in the propagation and polarisation directions. It appears that the fabric in the propagation direction dominates over the polarisation direction, as V_{xz} and V_{xy} are fastest while V_{yx} is slowest. The velocities V_{yz} and V_{zy}, for waves polarised in the symmetrical YZ plane, are nearly identical and fall in the middle of the range of the others. An electrical fault prevented the V_{zx} velocity from being obtained. The power coefficients are around 0.25 for V_{xy}, V_{yz} and V_{zy}, and 0.21 for V_{xz} and V_{yx} (Figure 8).

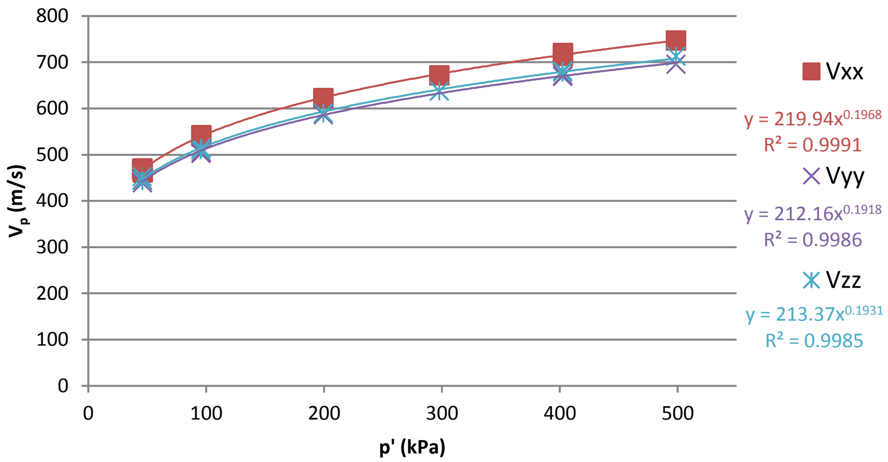

Figure 7: P-wave velocities with *p'* during isotropic loading.

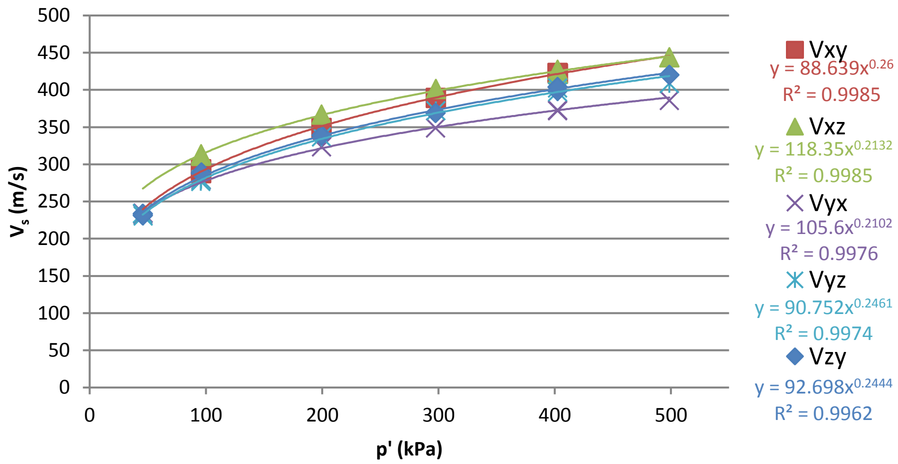

Figure 8: S-wave velocities with *p'* during isotropic loading.

3. Conclusions

This study presents recent developments in multiaxial testing that permit the combination of laboratory seismic testing with exploration of three-dimensional principal stress space. A Cubical Cell Apparatus with bender-extender piezoceramic elements fitted in all six faces are used so that wave propagation velocities of an analogue granular material can be determined. Understanding wave propagation through soils is essential for site response analysis in earthquake engineering, interpretation of geophysical surveys and SASW (Spectral Analysis of Surface Waves), interpretation of laboratory bender element tests, etc. The results of a first series of wave propagation tests for a sample of coarse, very poorly graded material under isotropic confinement showed some correlation between wave velocities and the sample stress-strain response. While P-wave velocity shows a direct relationship, with the stiffer axial stress-strain response corresponding to higher wave velocity, the S-wave behaviour appears to be controlled more by the fabric properties in the propagation direction than those in the polarization direction. The power law that links wave velocity to pressure shows power coefficients of 0.20 for P-waves and between 0.21 and 0.25 for S-waves.

Acknowledgements

Funding for this research was provided via EPSRC UK grant EP/G064180/1.

References

[1] B.O. Hardin and F.E. Richart. Elastic wave velocities in granular soils, *Journal of Soil Mechanics & Foundations Div.* ASCE, **89** (1963)

[2] D. J. Shirley and L. D. Hampton. Shear-Wave Measurementsin Laboratory Sediments. *Journal of the Acoustical Society of America*, Vol. 63, No. 2, (1978), 607–613

[3] P.J. Schultheiss. Simultaneous measurement of P and S wave velocities during conventional laboratory soil testing procedures. *Marine Geotechnology*, Vol 4, no 4, (1980), 343-367

[4] R. Dyvik and C. Madshus. Laboratory measurements of G_{max} using bender elements. Proc. ASCE Annual Convention: Advances in the art of testing soils under cyclic conditions, Detroit, Michigan, (1985), 186-197

[5] G. Viggiani and J.H. Atkinson. Interpretation of Bender Element Tests". *Géotechnique*, Vol. 45, No. 1, (1995), 149–154

[6] E.G.M. Brignoli, M. Gotti and J.H. Stokoe, Measurement of shear waves in laboratory specimens by means of piezoelectric transducers. *Geotechnical Testing Journal*, 19, (1996), 284-397

[7] D.S. Pennington, D.F.T. Nash, and M.L. Lings. Anistropy of G_0 Shear Stiffness in Gault Clay. *Géotechnique*, Vol. 47, No. 3, (1997), 391–398.

[8] S. Yamashita, T. Kawaguchi, Y. Nakata, T. Mikami, T. Fujiwara and S. Shibuya. Interpretation of international parallel test on the measurement of G_{max} using bender elements" *Soils and foundations*, 49(4), (2009), 631-650.

[9] M. Arroyo, D. Muir Wood, P. Greening, L. Medina and J. Rio. Effects of sample size on bender-based axial G0 measurements". *Géotechnique*, 56(1), (2006), 39-52.

[10] M.L. Lings and P.D. Greening. A novel bender/extender element for soil testing. *Géotechnique*, 51(8), (2001), 713-717

[11] J.-S. Lee and J.C. Santamarina. Bender Elements: Performance and Signal Interpretation. *Journal of Geotechnical and Geoenvironmental Engineering*, 131(9), (2005),1063-1070

[12] Ko, H.-Y. & Scott, R.F., 1967. Deformation of sand in shear. Journal of Soil Mechanics and Foundations Div ASCE

[13] Sadek, T., 2006. The Multiaxial Behaviour and Elastic Stiffness of Hostun Sand, PhD thesis. University of Bristol

[14] Cavarretta, I., O'Sullivan, C., Ibraim, E., Lings, M., Hamlin, S., & Muir Wood, D., 2012. Characterization of artificial spherical particles for DEM validation studies. Particuology, 10(2), pp.209–220

[15] J.F. Camenen, I. Cavarretta, S. Hamlin and E. Ibraim. Experimental and numerical assessment of a cubical sample produced by pluviation. *Géotechnique Letters*, 3(April-June), (2013), 44-51

[16] J.D. Goddard. Nonlinear elasticity and pressure-dependent wave speeds in granular media. *Proceedings Royal Society of London A: Mathematical and Physical Sciences* 430, (1990), 105–131